0026-895X/08/7303-801–812$20.00
MOLECULAR PHARMACOLOGY
Copyright © 2008 The American Society for Pharmacology and Experimental Therapeutics
Mol Pharmacol 73:801–812, 2008

Vol. 73, No. 3
40881/3294363
Printed in U.S.A.

Activity and Subcellular Trafficking of the Sodium-Coupled Choline Transporter CHT Is Regulated Acutely by Peroxynitrite

Metta Pinthong, Stefanie A. G. Black, Fabiola M. Ribeiro, Chumpol Pholpramool, Stephen S. G. Ferguson, and R. Jane Rylett

Department of Physiology and Pharmacology, Schulich School of Medicine and Dentistry, University of Western Ontario, London, Ontario, Canada (M.P., S.A.G.B., S.S.G.F., R.J.R.); Cell Biology Research Group, Robarts Research Institute, London, Ontario, Canada (M.P., S.A.G.B., F.M.R., S.S.G.F., R.J.R.); and Department of Physiology, Faculty of Science, Mahidol University, Bangkok, Thailand (M.P., C.P.)

Received August 15, 2007; accepted October 29, 2007

ABSTRACT

Excess formation of nitric oxide and superoxide by-products (peroxynitrite, reactive oxygen, and reactive nitrogen species) attenuates cholinergic transmission potentially having a role in Alzheimer disease pathogenesis. In this study, we investigated mechanisms by which acute exposure to peroxynitrite impairs function of the sodium-dependent hemicholinium-3 (HC-3)-sensitive choline transporter (CHT) that provides substrate for acetylcholine synthesis. The peroxynitrite generator 3-morpholinosydnonimine (SIN-1) acutely inhibited choline uptake in cells stably expressing FLAG-tagged rat CHT in a dose- and time-dependent manner, with an $IC_{50} = 0.9 \pm 0.14$ mM and $t_{1/2} = 4$ min. SIN-1 significantly reduced V_{max} of choline uptake without altering the K_m. This correlated with a SIN-1-induced decrease in cell surface CHT protein, observed as lowered levels of HC-3 binding and biotinylated CHT at the plasma membrane. It is noteworthy that short-term exposure of cells to SIN-1 accelerated the rate of internalization of CHT from the plasma membrane, but it did not alter return of CHT back to the cell surface. SIN-1 did not disrupt cell membrane integrity or cause cell death. Thus, the inhibitory effect of SIN-1 on choline uptake activity and HC-3 binding was related to enhanced internalization of CHT proteins from the plasma membrane to subcellular organelles.

The principal neurotransmitter used by cholinergic neurons is acetylcholine (ACh), which is synthesized by choline acetyltransferase (EC 2.3.1.6) from the precursors choline and acetyl-coenzyme A. The provision of sufficient choline is the rate-limiting step in synthesis of ACh under several conditions, with this choline being delivered into the nerve terminal by the sodium-coupled high-affinity choline transporter (Haga and Noda, 1973; Yamamura and Snyder, 1973) referred to as CHT (Okuda et al., 2000). Dysregulation and/or disruption of CHT function can profoundly affect the levels of ACh synthesized and released, thereby impairing cholinergic neurotransmission (Ferguson et al., 2004). CHT was cloned relatively recently (Okuda et al., 2000; Apparsundaram et al., 2001), and its regulation by phosphorylation (Gates et al., 2004) along with effects of modulation of its subcellular trafficking and compartmentalization on solute transport activity (Ferguson et al., 2003; Ribeiro et al., 2003, 2005, 2006) are active research topics.

Several studies link oxidative and nitrosative modifications of cellular constituents to the pathogenesis of neurodegenerative disorders such as Alzheimer disease (AD), Parkinson's disease, and sporadic amyotrophic lateral sclerosis. Peroxynitrite ($ONOO^-$) is a powerful oxidant that can be

This research was supported by operating grants to R.J.R. from the Alzheimer Society of Canada and Canadian Institutes for Health Research (CIHR). M.P. was funded by a Scholarship from the Higher Commission on Education, Ministry of Education of Thailand, as part of an exchange program between Mahidol University, Bangkok, Thailand, and the University of Western Ontario, London, Canada. S.A.G.B. is the recipient of a Doctoral Award from CIHR, and S.S.G.F. is a Career Investigator of the Heart and Stroke Foundation of Ontario and holds the Canada Research Chair in Molecular Neurobiology.

Article, publication date, and citation information can be found at http://molpharm.aspetjournals.org.

doi:10.1124/mol.107.040881.

ABBREVIATIONS: ACh, acetylcholine; CHT, high-affinity choline transporter protein; AD, Alzheimer disease; SIN-1, 3-morpholinosydnonimine; HEK, human embryonic kidney; FeTPPS, 5,10,15,20-tetrakissulfonatophenyl porphyrinato iron (III); FBS, fetal bovine serum; DCF, 2′,7′-dichlorofluorescein; DCFH, reduced 2′,7′-dichlorofluorescein; DCFH-DA, 2′,7′-dichlorofluorescein diacetate; SOD, superoxide dismutase; NHS, *N*-hydroxysuccinimide; RA, all-*trans* retinoic acid; KRH, Krebs-Ringer-HEPES; LDH, lactate dehydrogenase; MTT, [3-(4,5-dimethylthiazol-2-yl)-2,5-diphenyltetrazolium bromide]; PBS, phosphate-buffered saline; PBS/CM, phosphate-buffered saline with 0.1 mM $CaCl_2$ and 1 mM $MgCl_2$; CHAPS, 3-[(3-cholamidopropyl)dimethylammonio]propanesulfonate; PAGE, polyacrylamide gel electrophoresis; MesNa, sodium 2-mercaptoethanosulfonic acid; TfR, transferrin receptor.

formed in vivo from NO and superoxide anion (O_2^-) (Beckman, 1994). Because it is highly reactive, $ONOO^-$ can alter the structure and function of cellular proteins, lipids, and other macromolecules by oxidation or nitrosylation. Related to this, increased nitrotyrosine levels have been found in neuronal tissues in AD (Smith et al., 1997), suggesting that $ONOO^-$ may be involved in modifying protein function in this disorder.

Authentic $ONOO^-$, or $ONOO^-$ produced from 3-morpholinosydnonimine (SIN-1), profoundly inhibits activity of some neurotransmitter transporters, including the human 5-hydroxytryptamine transporter expressed heterologously in COS-7 cells (Bryan-Lluka et al., 2004) and the human dopamine transporter expressed in HEK 293 cells (Park et al., 2002). Inducing oxidative stress by treating cells with H_2O_2 also inhibits dopamine transporter, but this likely occurs by a different mechanism than inhibition caused by $ONOO^-$ (Huang et al., 2003). Oxidative stress mediated by the drug SIN-1 and $ONOO^-$, but not by H_2O_2, can affect high-affinity choline uptake activity in synaptosomes isolated from electric organ of *Torpedo marmorata* (Guermonprez et al., 2001). However, the mechanism by which $ONOO^-$ impairs choline transport was not investigated.

It was revealed recently that CHT proteins are located predominantly in intracellular compartments, with only a small proportion of total CHT being present at the cell surface (Lips et al., 2002; Okuda et al., 2002; Nakata et al., 2004; Ribeiro et al., 2005). Moreover, altering the relative subcellular localization and trafficking of CHT proteins between the plasma membrane and intracellular compartments seems to be a critical mechanism for regulating its activity (Apparsundaram et al., 2005; Ribeiro et al., 2005). In the present study, we investigated mechanisms by which oxidative stress mediated by the $ONOO^-$ generator SIN-1 modulates activity of rat CHT. We demonstrate for the first time that SIN-1 decreases choline uptake activity by changing the dynamics of CHT proteins at the cell surface by modifying their internalization and cycling between the cell surface and subcellular compartments.

Materials and Methods

Materials. SIN-1 was from BIOMOL Research Laboratories (Plymouth Meeting, PA); 5,10,15,20-tetrakissulfonatophenyl porphyrinato iron(III) (FeTPPS) was from Calbiochem (San Diego, CA); and [*methyl*-^{3}H]choline chloride (86 Ci/mmol) and [*methyl*-^{3}H]hemicholinium-3 diacetate (125 Ci/mmol) were obtained from PerkinElmer Life and Analytical Sciences (Waltham, MA). EZ-Link sulfo-NHS-SS-biotin and immobilized NeutrAvidin beads were from Pierce Biotechnology (Rockford, IL). All others chemical were from Sigma-Aldrich (St. Louis, MO). SH-SY5Y neuroblastoma cells were purchased from American Type Culture Collection (Manassas, VA), HEK 293 Flp-In cells and all cell culture media, fetal bovine serum (FBS), and reagents were from Invitrogen Canada Inc. (Burlington, ON, Canada). Rabbit polyclonal and mouse monoclonal anti-nitrotyrosine antibodies were obtained from Upstate Biotechnology (Charlottesville, VA). Protein A-Sepharose and 2′,7′-dichlorofluorescein diacetate (DCFH-DA) were from Sigma Diagnostics Canada (Mississauga, ON, Canada). Enhanced chemiluminescence immunoblotting reagents were from GE Healthcare Life Sciences (Baie d'Urfé, QC, Canada). The polyclonal antibody against CHT was raised in rabbits by Genemed Synthesis (San Francisco, CA) using a peptide encoding 16 residues (DVDSSPEGSGTEDNLQ) that are conserved at the carboxyl terminus of human and rat CHT as immunogen; the peptide was conjugated to keyhole limpet hemocyanin carrier protein by an amino-terminal cysteine. CHT-specific immunoglobulins were affinity-purified in our laboratory from the crude antiserum on NHS-Sepharose (GE Healthcare) to which the antigenic peptide had been coupled as the binding element. The specificity of this antibody for detection of CHT was described previously by Ribeiro et al. (2005).

Stable Transfection and Selection of HEK 293 and SH-SY5Y Cells. A FLAG epitope-tag (DYKDDDDK) was added to the amino terminus of rat CHT by polymerase chain reaction (Ribeiro et al., 2005); the full-length cDNA for CHT ligated to pSPORT was obtained as a gift from Dr. Takashi Okuda (University College London, London, UK) (Okuda et al., 2000). HEK 293 cell lines stably expressing FLAG-tagged CHT (referred to as HEK 293-CHT cells) were prepared by introducing FLAG-CHT ligated to pcDNA5 into the Flp recombinase target site in HEK-Flp-In cells using Lipofectamine 2000 (Invitrogen Canada Inc.) transfection. Cells were grown in Dulbecco's modified Eagle medium with 10% FBS, 0.1% gentamicin, and 50 μg/ml hygromycin B to select stable transformants. SH-SY5Y neuroblastoma cells were transfected with FLAG-tagged rat CHT ligated into pcDNA3.1(−) using Lipofectamine 2000. Stable transformants (referred to as SH-SY5Y-CHT cells) were selected with 500 μg/ml G-418 (Geneticin; Invitrogen Canada Inc.) for 4 weeks, and subsequently they were maintained in Dulbecco's modified Eagle medium, 10% FBS, 0.1% gentamicin, and 100 μg/ml G-418. Differentiation of SH-SY5Y-CHT cells was induced by supplementing culture media with 10 μM all-*trans*-retinoic acid (RA) for at least 3 days.

[^{3}H]Choline Uptake Assay. Cells were washed with Krebs-Ringer-HEPES (KRH) buffer, pH 7.4 (124 mM NaCl, 5 mM KCl, 1.5 mM $CaCl_2$, 1.2 mM $MgCl_2$, 10 mM glucose, and 20 mM HEPES), and then they were incubated at 37°C in the absence or presence of SIN-1 for times specified under *Results*. After the treatment period, warm KRH buffer containing [^{3}H]choline (0.5 μM; 0.4 Ci/mmol) was added, and incubation was continued for 5 min. For kinetic analysis, choline uptake was measured over a range of choline concentrations between 0.5 and 10 μM, with the specific activity of [^{3}H]choline held constant at 0.4 Ci/mmol. [^{3}H]Choline uptake was terminated by rapidly washing the cells twice with ice-cold KRH. Cells were solubilized in 0.1 N NaOH for 30 to 60 min, and then an aliquot was removed for measurement of radioactivity by liquid scintillation spectrometry. Additional aliquots of the solubilized samples were used for quantification of sample protein content using Protein Assay Dye Reagent (Bio-Rad Laboratories, Hercules, CA). HC-3-sensitive [^{3}H]choline uptake was determined by subtracting choline uptake in the presence of HC-3 from total choline uptake and normalizing to sample protein content to be expressed as picomoles per milligram of protein per 5 min.

Cell Toxicity Assays. Lactate dehydrogenase (LDH) activity was measured spectrophotometrically in aliquots of cell lysates or culture medium to determine whether drug treatments resulted in changes in plasma membrane integrity of cells. LDH activity was monitored as a change in absorbance at 340 nm due to the loss of NADH caused by the reduction of pyruvate to lactate coupled to the oxidation of NADH to NAD^+ as described previously (Baskey et al., 1990). Cells on 12-well plates were treated with SIN-1 at 10, 100, or 1000 μM for 45 min in KRH buffer, pH 7.4, at 37°C. Culture medium was collected for measurement of LDH release from cells, and then cells were lysed in 0.5 ml of 1% Triton X-100 to measure total cellular LDH levels. Released LDH activity in culture medium was expressed as a percentage of total cellular LDH activity. Changes in NADH level in assay solutions were monitored at 340 nm at 30-s intervals for 5 min. The colorimetric 3-(4,5-dimethylthiazol-2-yl)-2,5-diphenyltetrazolium bromide (MTT) assay was used to determine whether drug treatments compromised cell viability as described by Calderón et al. (1999). Cells in 96-well plates were washed with warm KRH buffer, and then they were incubated in the presence or absence of SIN-1 for 45 min at 37°C. After incubation of control and treated cells with MTT, cells were rinsed and allowed to air dry before dissolving in 100 μl of 0.04% HCl in isopropanol. The amount of formazan

reaction product formed in each well was determined by measuring absorbance at 570 nm. Negative control wells contained medium alone with no cells. The viability of treated cells was presented as a percentage of control vehicle-treated cells.

[^{3}H]HC-3 Binding. Cells were preincubated at 37°C for 45 min in KRH buffer with the addition of vehicle or varying doses of SIN-1, and then they were washed twice with ice-cold KRH and maintained on ice for 10 min. Subsequently, cells were incubated in KRH buffer containing 10 nM [^{3}H]HC-3 (23 Ci/mmol) in the absence (total binding) or presence (nonspecific binding) of 1 μM unlabeled HC-3 for 1 h at 4°C. Cells were then washed rapidly twice with ice-cold KRH to remove unbound [^{3}H]HC-3, and finally they were digested with 0.1 N NaOH. Aliquots of each sample were taken for radioactivity measurement by liquid scintillation spectrometry and for protein quantification. Specific binding was determined as the difference between total binding and nonspecific binding, and it was normalized to sample protein content to be expressed as femtomoles per milligram of protein per hour.

Cell Surface Protein Biotinylation Assay. Cells were treated with vehicle or SIN-1 in KRH buffer at 37°C at doses and times indicated under *Results*, and then plasma membrane proteins were biotinylated as described previously (Ribeiro et al., 2005). In brief, cells were washed three times with ice-cold PBS/CM (PBS containing 0.1 mM $CaCl_2$ and 1 mM $MgCl_2$), and then they were incubated with 1 mg/ml sulfo-NHS-SS-biotin in PBS/CM for 1 h at 4°C. Unbound sulfo-NHS-SS-biotin was quenched by washing and incubating cells with 100 mM glycine in ice-cold PBS/CM, followed by washing twice with PBS/CM. Subsequently, biotinylated cells were lysed for 30 min at 4°C in buffer comprised of 1% CHAPS, 0.1 M sodium phosphate buffer, pH 7.2, 10% glycerol, and 150 mM NaCl supplemented with 700 U/ml DNase and protease inhibitors [1 mM 4-(2-aminoethyl)benzenesulfonyl fluoride, 10 μg/ml each of aprotinin and leupeptin, and 25 μg/ml pepstatin A]. Aliquots of total cell lysates were incubated at 4°C with NeutrAvidin beads for 2 h with gentle mixing. The beads were then washed with lysis solution, and proteins were eluted from the beads with SDS sample buffer (2% SDS, 10% glycerol, 0.1 M sodium phosphate buffer, pH 7.2, 0.001% bromphenol blue, and 2.5% β-mercaptoethanol) for 5 min at 60°C. Aliquots of biotinylated (avidin-bound) proteins, nonbiotinylated proteins, and total cell lysates were separated by SDS-PAGE, and then proteins were transferred to polyvinylidene difluoride membranes. The membranes were blocked with 8% nonfat dry milk in wash buffer (PBS and 0.1% Tween 20) for 30 min, and then they were incubated for 2 h with anti-CHT antibody (1:1000) in wash buffer containing 8% milk. After washing, the membranes were incubated with peroxidase-conjugated anti-rabbit IgG secondary antibody diluted 1:10,000 for 1 h in wash buffer containing 8% milk. Excess antibody was removed by washing, and membranes were processed for chemiluminescence detection using the ECL kit (GE Healthcare). Immunoreactive bands were quantified by densitometry using Scion Image software made available by National Institutes of Health (http://rsb.info.nih.gov/nih-image).

Internalization and Recycling of CHT in Cells. After the biotinylation of plasma membrane proteins, cells were treated rapidly with either vehicle or 1 mM SIN-1 in warm KRH buffer, and then they were transferred to 37°C for varying times to monitor internalization of cell surface proteins. Protein internalization was terminated by transferring culture dishes to 4°C and washing twice with ice-cold PBS/CM. Cells were treated with the membrane-impermeable reducing agent sodium 2-mercaptoethanosulfonic acid (MesNa; 50 mM) in TE buffer (150 mM NaCl, 1 mM EDTA, 0.2% bovine serum albumin, and 20 mM Tris-HCl, pH 8.6) to strip biotin from biotinylated proteins that had not undergone internalization and that were retained at the cell surface. For each experiment, the biotin stripping efficiency was assessed on a plate of cells that was treated in parallel but that had been kept on ice to block internalization of cell surface proteins. In experiments designed to assess the movement of previously internalized biotinylated CHT back to the plasma membrane ("recycling"), biotinylated cell surface proteins were allowed to undergo internalization by incubating cells at 37°C for 15 min, and then the cells were transferred to 4°C and residual biotin was stripped from proteins that remained at the cell surface. Subsequently, cells were returned to a second round of incubation at 37°C in KRH buffer to allow return of internalized biotinylated proteins to the plasma membrane. Treatments in the presence or absence of SIN-1 were initiated at this latter step for times specified under *Results*. Finally, biotin was removed from previously internalized biotinylated CHT proteins that had returned (recycled) to the cell surface using MesNa in TE buffer as described above, thereby allowing measurement of biotinylated proteins retained within the cells. Biotinylated proteins were separated from nonbiotinylated proteins on NeutrAvidin beads, and then they were analyzed by SDS-PAGE and immunoblotting as described above.

Detection of Tyrosine Nitration in CHT. HEK 293-CHT cells were harvested, and aliquots containing 1×10^6 cells were transferred to microcentrifuge tubes. Cells were then washed with PBS and resuspended in KRH buffer, after which SIN-1, authentic $ONOO^-$, or vehicle was added with immediate mixing. After 30-min incubation at room temperature, cells were washed three times with PBS, and then they were centrifuged and lysed in CHAPS buffer containing protease inhibitors as described above. Immunoprecipitation was used to test for the presence of CHT-containing nitrotyrosine residues in total cell lysates as described by Tran et al. (2003). In brief, 50 μl of protein A-Sepharose beads was incubated overnight with either rabbit polyclonal anti-nitrotyrosine antibody (1:125) or mouse anti-FLAG antibody (1:125). Subsequently, aliquots of antibody-bound protein A-Sepharose were added to cell lysates (400–500 μg of protein) and incubated overnight at 4°C. Antigen-antibody complexes were recovered by centrifugation, and bound proteins were eluted in double-strength SDS sample buffer with heating at 60°C for 5 min. Proteins were separated by SDS-PAGE, and probed with mouse monoclonal anti-nitrotyrosine antibody (1:1000), or rabbit polyclonal anti-CHT antibody (1:2000), or rabbit polyclonal anti-nitrotyrosine antibody (1 μg/ml); information from these two forms of immunoblot were compared with evaluate whether CHT contained nitrotyrosine residues.

2′7′-Dichlorfluorescein Assay. HEK 293-CHT and SH-SY5Y-CHT cells were seeded in 96-well plates at 5×10^4 cells/well and 1×10^5 cells/well, respectively. On the day of the experiments, cells were incubated with KRH containing 50 μM DCFH-DA for 1 h at 37°C, and then media were aspirated and cells were washed once to remove extracellular DCFH-DA. Cell-permeable DCFH-DA taken up by the cells is converted by intracellular esterases to DCFH by removal of the diacetate moiety. SIN-1, H_2O_2, or vehicle was added to duplicate wells, and fluorescence intensity changes related to oxidation of DCFH to DCF were followed at 5-min intervals for 30 min (λ_{Ex} = 485 and λ_{Em} = 510 nm). This assay was also used to test whether SOD, catalase, and FeTPPS could reduce DCFH oxidation in cells by adding these agents to culture wells 5 min before the addition of H_2O_2, SIN-1, or vehicle. Changes in fluorescence were calculated by the equation $\Delta F = (F_{t30} - F_{t0})/F_{t0} \times 100$.

Membrane Potential Measurements. Effects of SIN-1 on membrane potential of SH-SY5Y cells was monitored with the membrane potential-dependent fluorescent dye Oxonal V, as described by Kukkonen et al. (1996). In brief, cells were harvested in PBS containing 0.02% EDTA, and then they were centrifuged and washed once with Ca^{2+}-free KRH buffer. Cell pellets were resuspended in KRH containing 0.5 μM bis-oxonal, and then they were incubated for 30 min in the dark at 25°C with gentle mixing to allow loading of dye into cells. Subsequently, aliquots of cell suspension were placed in a stirred cuvette holder heated at 37°C of a fluorescence spectrophotometer (PTI, South Brunswick, NJ), and fluorescence (λ_{Ex} = 490 and λ_{Em} = 530 nm) was monitored as a function of time. Vehicle or drug (1 mM SIN-1 or 1 mM ouabain) was added at about 5 min when the baseline had stabilized. At the end of each recording, 10 μM gramicidin was added to the cells to induce maximal depolarization for measurement of the maximum fluorescence emission. Changes in

fluorescence indicative of changes in membrane potential of the cells were calculated by $\Delta F = (F_{t30} - F_{t0})/F_{t0} \times 100$.

Data Analysis. Data are plotted as mean ± S.E.M., with the number of independent experiments performed shown as *n* values in the figure legends. Prism 4 and InStat software (both from GraphPad Software Inc., San Diego, CA) were used to perform statistical analyses. For nonlinear regression curve-fitting, one-site competition and one-phase exponential decay were used to determine the IC_{50} and $t_{1/2}$ values of dose-response and maximal inhibition of choline uptake, respectively. Sigmoid and Michaelis-Menten equations were used to fit dose-response curves and to calculate kinetic parameters (V_{max} and K_m) of choline uptake, respectively. Statistical significance was determined using either unpaired Student's *t* test or one-way analysis of variance with Dunnett's post hoc multiple comparison test, as appropriate.

Results

SIN-1 Decreased CHT Activity. To begin, the effect of SIN-1 on CHT was assessed by measuring HC-3-sensitive, high-affinity choline uptake activity in HEK 293-CHT cells. These experiments revealed that SIN-1 significantly decreases CHT activity in a dose-dependent manner, with an IC_{50} of 0.9 ± 0.14 mM (Fig. 1A). The onset of this inhibition is rapid. Cells were incubated in the presence of 1 mM SIN-1 for up to 120 min with maximal inhibition of choline uptake developing with a $t_{1/2}$ of approximately 4 min. It is noteworthy that the inhibitory effect of SIN-1 plateaus at approximately 50% of control levels, and it remains constant for up to 120 min (Fig. 1B). Unlike SIN-1, treatment of cells with 1 mM H_2O_2 does not alter CHT activity (Fig. 1A).

To determine whether the inhibitory effect of SIN-1 on CHT activity is cell type-specific, we developed lines of SH-SY5Y neuroblastoma cells that stably express FLAG-tagged rat CHT (SH-SY5Y-CHT cells) for comparison with the HEK 293-CHT cells. As illustrated in Fig. 2A, compared with wild-

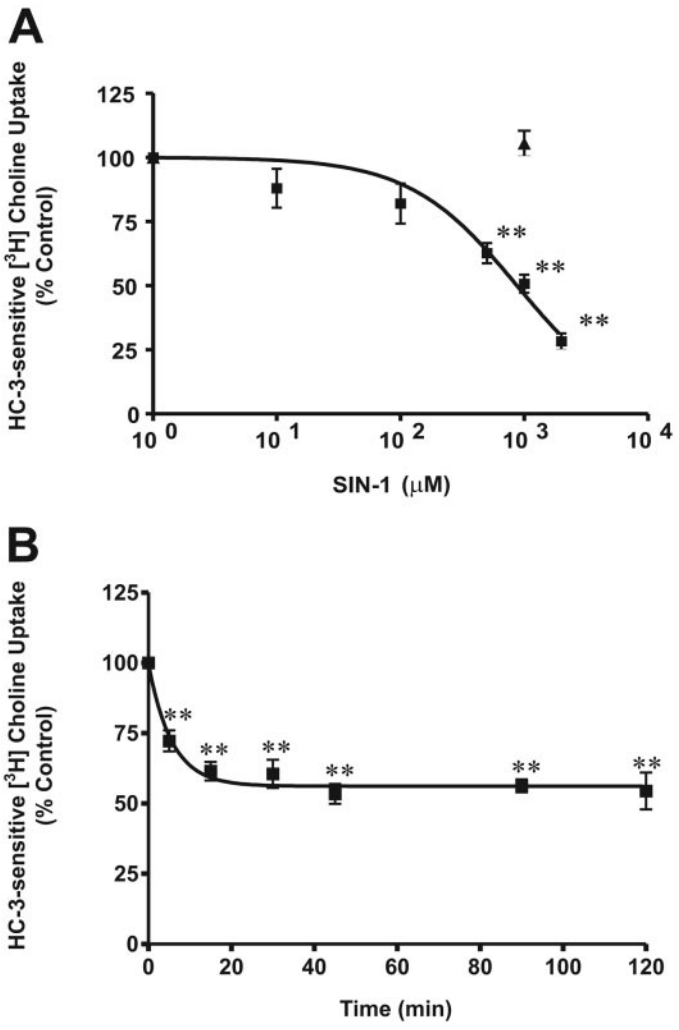

Fig. 1. Acute exposure of HEK 293-CHT cells to SIN-1 inhibits HC-sensitive choline uptake. A, cells were preincubated with various concentrations of SIN-1 (10 μM–2 mM) (■) or with 1 mM H_2O_2 (▲) for 45 min, and for various times (5–120 min) (B) before choline uptake activity was measured at 0.5 μM [^{3}H]choline. Data from SIN-1-treated cells are normalized to that obtained for control (vehicle-treated) cells (percentage of control), and they are expressed as the mean ± S.E.M. of three to five independent experiments with triplicate measurements in each experiment. Statistically significant differences between control and SIN-1-treated cells are denoted as **, $p < 0.01$.

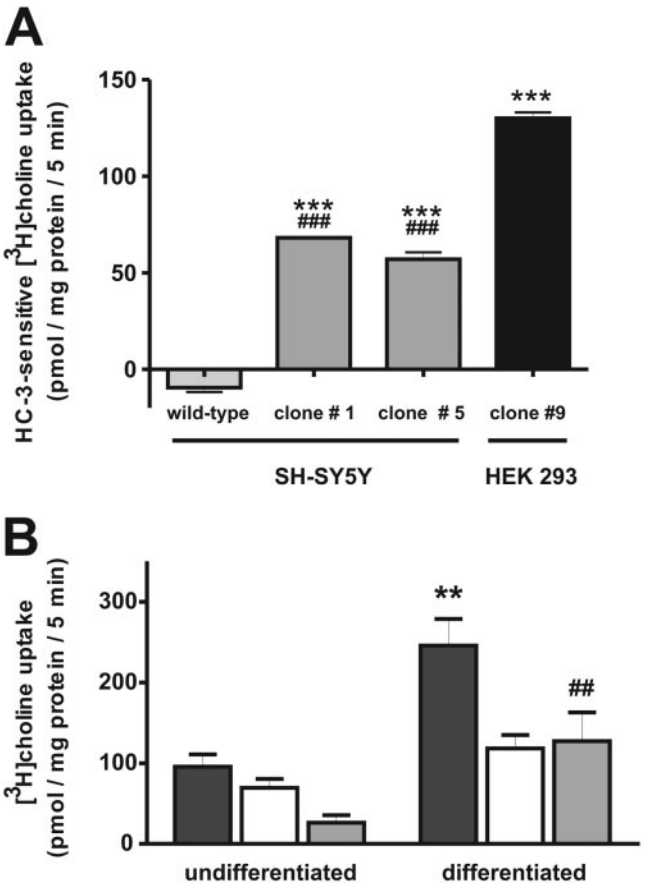

Fig. 2. SH-SY5Y-CHT cells express HC-3-sensitive choline uptake that increases with differentiation. A, two SH-SY5Y-CHT cell lines were tested, revealing CHT activity at approximately 50% of that found in HEK 293-CHT cells. Wild-type SH-SY5Y cells do not express HC-3-sensitive choline uptake activity constitutively. ***, $p < 0.001$ compared with wild-type cells; ###, $p < 0.001$ compared with HEK 293-CHT cells. B, differentiation of SH-SY5Y-CHT cells with retinoic acid treatment for 3 days enhances total (black bars), but not HC-insensitive (white bars), choline uptake activity. Net HC-sensitive, CHT-mediated choline uptake was approximately 5-fold greater in differentiated cells [127.28 ± 17.76 pmol/mg/5 min] compared with undifferentiated cells [26.05 ± 4.68 pmol/mg/5 min]. Data are expressed as mean ± S.E.M. ($n = 4$ independent experiments). Total choline uptake in differentiated cells was statistically different from that measured in undifferentiated cells and from HC-insensitive choline uptake in both differentiated and undifferentiated cells, denoted as **, $p < 0.01$. Total choline uptake in undifferentiated cells and HC-insensitive uptake in differentiated and undifferentiated cells were not significantly different from each other.

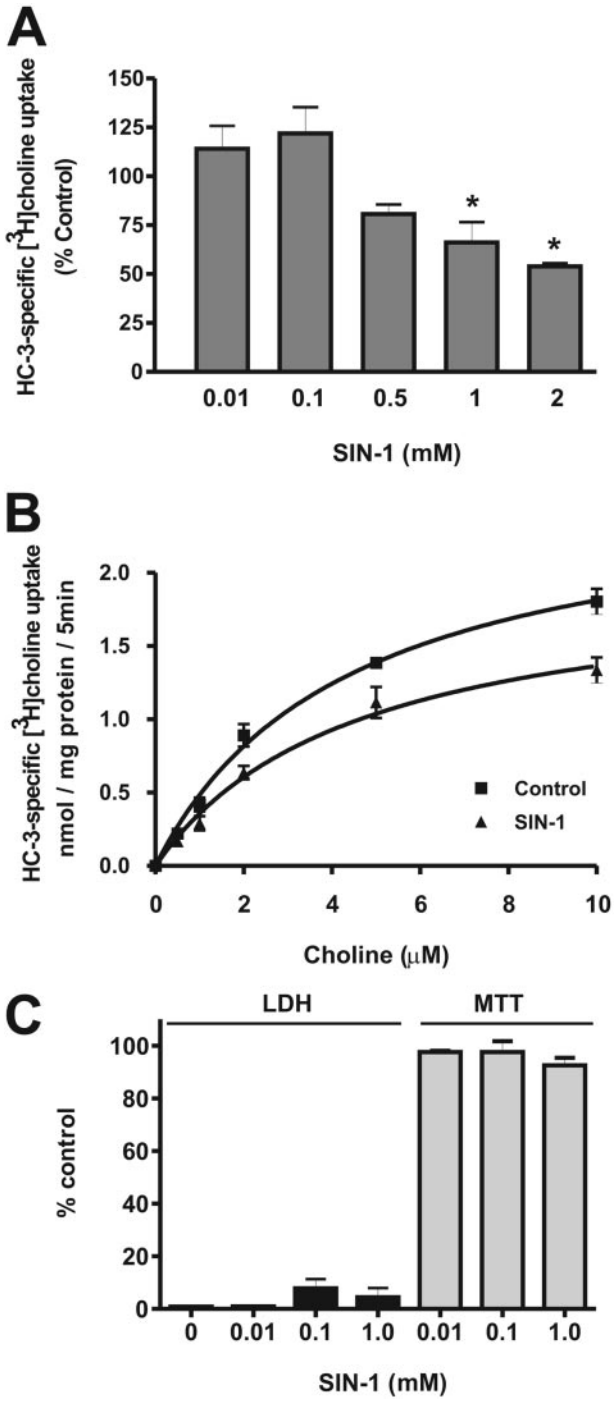

Fig. 3. SIN-1 inhibits CHT activity in differentiated SH-SY5Y cells. A, [^{3}H]choline uptake was inhibited in a dose-dependent manner in cells treated for 30 min with SIN-1 at concentrations between 10 μM and 2 mM. Data for SIN-1-treated cells are expressed as percentage of vehicle-treated controls, and they are graphed as mean ± S.E.M. ($n = 4$). Statistically significant differences compared with control are indicated by *, $p < 0.05$ (one-way analysis of variance with post hoc Dunnett's multiple comparison test). B, kinetic parameters for HC-3-sensitive [^{3}H]choline uptake in control and SIN-1-treated differentiated SH-SY5Y-CHT cells were estimated using [^{3}H]choline concentrations between 0.5 and 10 μM in the absence or presence of 1 μM HC-3. Data are calculated as nanomoles per milligram of protein per 5 min, and they are expressed as mean ± S.E.M. from five independent experiments with duplicate measurements. Choline uptake data are plotted as a function of [^{3}H]choline concentration, with curves fitted by nonlinear regression analysis using GraphPad Prism 4. SIN-1 (30 min; 1 mM) decreased the V_{max} of choline uptake by 25% (*, $p < 0.05$), with no significant change in K_m. C, effect of SIN-1 treatment on plasma membrane integrity and cell viability was tested by monitoring LDH release from cells and MTT metabolism, respectively. As shown, treatment of cells for 30 min with SIN-1 up to a concentration of 1 mM did not significantly alter either of these measures compared with vehicle-treated control cells. Data are expressed as mean ± S.E.M. from at least three independent experiments.

type SH-SY5Y cells, two separate SH-SY5Y-CHT cell lines that were tested displayed substantial HC-sensitive choline uptake activity; this activity was approximately 50% less than that measured in parallel cultures of HEK 293-CHT cells because of lower levels of expression of the transgene in the neural cell lines (data not shown). SH-SY5Y cells grown in the presence of RA differentiate morphologically with the extension of neuritic processes and increased expression of neuron-specific markers (Encinas et al., 1999; Truckenmiller et al., 2001). It is noteworthy that HC-sensitive CHT activity was increased significantly by approximately 5-fold in RA-differentiated SH-SY5Y-CHT cells compared with undifferentiated SH-SY5Y-CHT cells ($p < 0.01$) (Fig. 2B). HC-insensitive choline uptake was not statistically different between undifferentiated and differentiated cells. As illustrated in Fig. 2B, HC-insensitive choline uptake accounts for approximately 75% of total choline uptake in undifferentiated cells compared with approximately 50% of total uptake in differentiated cells. The mechanisms underlying this are not clear, but it does not relate to changes in steady-state levels of CHT mRNA in the cells (data not shown).

Importantly, we determined that SIN-1 also decreases [^{3}H]choline uptake activity in RA-differentiated SH-SY5Y-CHT cells, with the magnitude of effect being similar to that observed in the HEK 293-CHT cells (Fig. 3A). Moreover, neither 1 mM H_2O_2 nor the NO donor 1-hydroxy-2-oxo-3-(3-aminopropyl)-3-isopropyl-1-triazene (1 mM) suppress [^{3}H]-choline uptake in these CHT-expressing cell models (data not shown). Information about the mechanism by which SIN-1 affects CHT activity was obtained by measuring the kinetic parameters of [^{3}H]choline uptake in vehicle and SIN-1-treated RA-differentiated SH-SY5Y-CHT cells. These experiments reveal that the V_{max} for choline uptake is reduced significantly from 2.63 ± 0.15 to 2.02 ± 0.13 nmol/mg of protein/5 min in vehicle- and SIN-1-treated (1 mM; 30 min) cells, respectively (decrease to 75% of control value; $p < 0.05$, unpaired t test) (Fig. 3B). The apparent K_m values established for choline uptake in vehicle- and SIN-1-treated cells do not differ significantly (4.46 ± 0.48 and 5.12 ± 0.89 μM, respectively) (Fig. 3B). It is possible, however, that this effect on choline uptake could be due to cellular damage or toxicity induced by SIN-1. Consequently, we used the MTT assay to monitor cell viability and the release of cytoplasmic LDH into cell culture medium to detect changes in plasma membrane integrity. No differences were found between control and SIN-1-treated cells in either the MTT assay or in LDH levels in the culture medium, thereby establishing that SIN-1 does not compromise cell viability under these experimental conditions (Fig. 3C).

Based on the finding that SIN-1 leads to a rapid and substantial loss of choline uptake activity in CHT-expressing cells, we carried out experiments designed to address three potential mechanisms: 1) changes in the density of transport proteins located at the cell surface, 2) nitration of susceptible tyrosine residues in CHT leading to loss-of-function, or 3) loss of the driving force for choline transport by collapse of the

plasma membrane sodium electrochemical gradient or membrane potential.

Effect of SIN-1 on Cell Surface Levels of CHT. For CHT to exert its function of transporting choline into the neuron, it must be inserted into the plasma membrane. Thus, we hypothesized that the SIN-1-induced decrease in choline uptake activity is related to a decrease in the density of CHT proteins at the plasma membrane. To test this, we exposed HEK 293-CHT cells to 1 mM SIN-1 to decrease choline uptake activity by approximately 50%, and then we measured the levels of CHT at the cell surface in comparison with vehicle-treated control cells. For this purpose, we used the well-characterized high-affinity choline uptake antagonist HC-3 as a ligand in binding assays because it binds competitively to CHT, but it is not a solute for the transporter (Chatterjee et al., 1987). Moreover, these assays were carried out at 4°C to block internalization of CHT proteins from the cell surface to intracellular compartments (Ribeiro et al., 2005). As illustrated in Fig. 4, these experiments revealed that specific binding of a saturating concentration of [^{3}H]HC-3 is decreased in 1 mM SIN-1-treated cells to approximately 50% of the control levels ($p < 0.01$). Furthermore, at a lower dose (0.1 mM), SIN-1 also significantly decreases [^{3}H]HC-3 binding to approximately 75% of control levels ($p < 0.01$), which corresponds well with the choline uptake data (data not shown).

To corroborate this finding, we used a second approach to quantify cell surface levels of CHT protein and to assess changes after SIN-1 treatment. In these studies, plasma membrane proteins were biotinylated and recovered on NeutrAvidin beads, and then CHT was detected and quantified by immunoblotting with anti-CHT antibody (Ribeiro et al., 2005). To begin, we assessed the effect of SIN-1 treatment on the size of the pool of CHT proteins that becomes biotinylated in HEK 293-CHT cells that were incubated at 37°C for varying times with either vehicle or 1 mM SIN-1 during protein biotinylation. In this experimental paradigm, biotinylated CHT may be located at the cell surface, internalized to subcellular organelles after labeling, or internalized and subsequently returned to the plasma membrane. This combined pool of CHT, termed the recycling pool, is a subpopulation of the total cellular CHT proteins, and it is available for trafficking between cell surface and subcellular organelles to regulate choline uptake activity by fine-tuning plasma membrane CHT levels (Ribeiro et al., 2006). Figure 5A shows a representative immunoblot, and it reveals that SIN-1 substantially reduces the total size of the recycling pool of CHT proteins in a time-dependent manner (Fig. 5, A and B). It is also clear from Fig. 5B that the kinetics of biotinylation of CHT proteins in the recycling pool differs in vehicle-treated compared with SIN-1-treated cells; over a 60-min time course, the rate and magnitude of biotinylation of this CHT pool is greater in control cells compared with cells exposed to SIN-1.

It is important to note from the immunoblot of CHT in Fig. 5A that despite having a calculated molecular mass of approximately 63 kDa, CHT become visible on immunoblots as

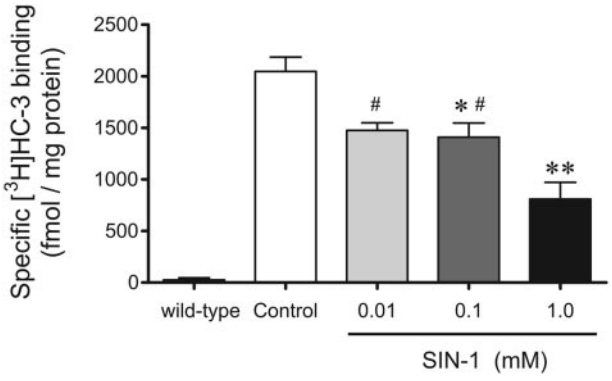

Fig. 4. SIN-1 decreases the binding of [^{3}H]HC-3 to CHT in HEK 293-CHT cells. Cells were treated for 45 min with vehicle or SIN-1 (0.01, 0.1, and 1 mM) before measuring total binding of [^{3}H]HC-3 using 10 nM ligand in the absence or presence of 1 μM HC-3 for estimation of nonspecific binding. Wild-type HEK 293 cells do not express CHT constitutively as seen by the lack of specific [^{3}H]HC-3 binding. Specific binding was determined as the difference between total binding and nonspecific binding, with data normalized to sample protein content. Data are expressed as femtomoles of [^{3}H]HC-3 bound per milligram of protein, and they are graphed as mean ± S.E.M. from five independent experiments with duplicate determinations. Statistically significant differences compared with control group are indicated by *, $p < 0.05$ or **, $p < 0.01$. Statistically significant differences compared with 1 mM SIN-1 treatment group are indicated by #, $p < 0.05$.

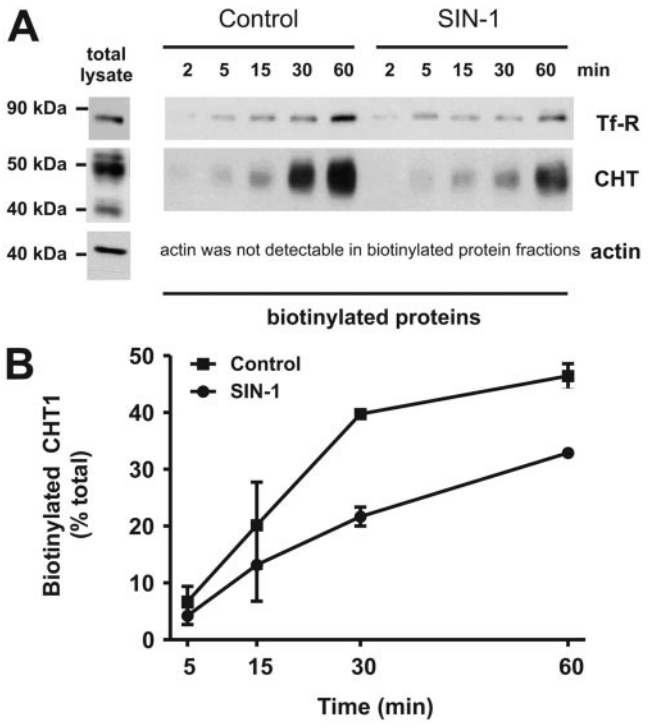

Fig. 5. SIN-1 treatment decreases the size of the total recycling pool of CHT in HEK 293-CHT cells. A, cells were incubated for varying times at 37°C in the absence or presence of 1 mM SIN-1 in buffer containing sulfo-NHS-SS-biotin to biotinylate CHT proteins when they are present at the cell surface. A representative immunoblot (middle) shows total biotinylated CHT proteins located at the cell surface and internalized into subcellular compartments; total cellular CHT content (nonbiotinylated and biotinylated) (left lane, middle). A representative immunoblot showing biotinylated TfR is shown for the same experimental paradigm (top) with total TfR in cell lysate illustrated in the left lane, top. Actin immunoreactivity in the biotinylated protein fractions was used as a negative control. The absence of actin in these fractions (bottom) indicates that CHT or TfR present is recovered as solubilized biotinylated membrane proteins isolated on NeutrAvidin beads, rather than from contamination of the fractions by intact membranes. Actin immunoreactivity in cell lysates is shown in the left lane, bottom. B, a line graph summarizes time course data from densitometric profiles of the biotinylated CHT pool in control and SIN-1-treated cells normalized to total cellular CHT for five independent experiments.

at least one, and often two or three, bands with masses of approximately 40, 50, and 80 kDa. The 50-kDa protein is the predominant species, with the relative abundance of immunoreactive CHT bands varying depending on expression levels of CHT in cells. As shown in Fig. 5A (middle, left), in HEK 293-CHT cell lysates, immunoreactive CHT proteins are observed with masses of approximately 40 and 50 kDa. It is noteworthy that biotinylated CHT protein (Fig. 5A, middle, right) corresponds to the 50-kDa immunoreactive CHT protein. Also included in this experiment for comparison with CHT was assessment of the effects of SIN-1 on another cell surface receptor, the transferrin receptor (TfR), which is known to undergo clathrin-mediated internalization (Hanover et al., 1985). As illustrated in Fig. 5A (top), SIN-1 also substantially reduces the total size of the biotinylated pool of TfR in a time-dependent manner similar to that observed for CHT.

As shown in Fig. 6A (left), SIN-1 significantly decreases the amount of CHT immunoreactivity at the plasma membrane in a dose-dependent manner. This decrease in CHT density at the cell surface develops rapidly with reduced immunoreactivity seen in cells treated with 1 mM SIN-1 for only 5 min compared with vehicle-treated control cells. There was no change in the total cellular levels of CHT protein between control and SIN-1-treated cells, as illustrated by the immunoblots in Fig. 6A (bottom). Quantification of these data from multiple independent experiments by densitometry shows that the level of CHT present at the plasma membrane was reduced to approximately 60 and 75% of control in cells treated for 45 min with 1 and 0.1 mM SIN-1, respectively ($p < 0.01$) (Fig. 6B). SIN-1 treatment had no apparent

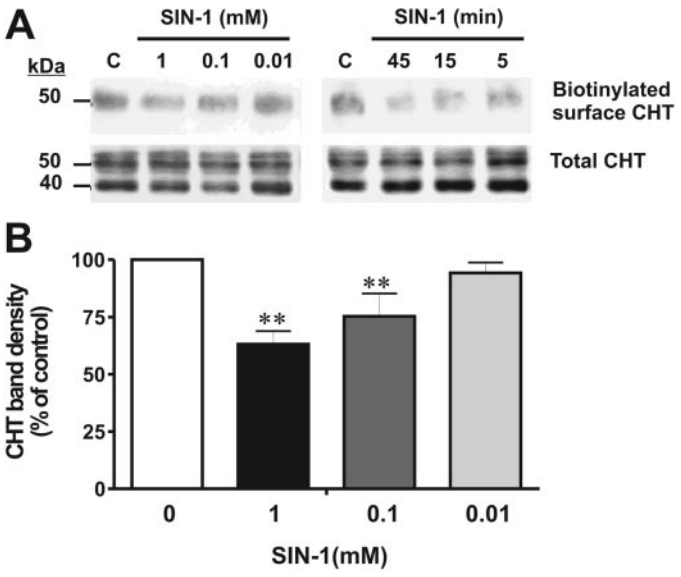

Fig. 6. SIN-1 treatment decreases the amount of CHT protein at the cell surface. A, HEK 293-CHT cells were incubated at 37°C for 45 min in the absence or presence of SIN-1 (0.01, 0.1, or 1 mM) (top, left) or with 1 mM SIN-1 for 5, 15, or 45 min (top, right) before biotinylation of cell surface proteins at 4°C for 1 h. Aliquots of lysates (10 μg of protein) from parallel sets of cells not undergoing biotinylation were immunoblotted to assess total CHT levels (bottom). B, immunoblots of biotinylated CHT were quantified by densitometry and relative absorbance units for band densities from SIN-1-treated cells are expressed as a percentage of cell surface CHT obtained for vehicle-treated control cells. Data shown are from three to five independent experiments, and they represent mean ± S.E.M. Asterisks (**) indicate that data are statistically different from controls at the level of $p < 0.01$.

effect on actin levels on immunoblots of total cell lysates, and actin was not detectable in the biotinylated protein fractions (data not shown). These latter findings validate the methodology by indicating further that plasma membrane integrity was maintained in SIN-1-treated cells and that only cell surface proteins are biotinylated.

SIN-1 Enhances the Internalization of CHT from the Cell Surface. Although it was predicted initially that CHT proteins would be localized mostly to the plasma membrane from where they transport choline into the cell, it is clear that unlike some other neurotransmitter transporters CHT is distributed primarily in intracellular compartments with only a small proportion at the cell surface. Moreover, CHT present at the cell surface is internalized rapidly into intracellular membranous organelles through the endocytic endosomal pathway (Ribeiro et al., 2006). Thus, it is expected that the steady-state plasma membrane level of CHT protein will be determined by the rates at which it is internalized into subcellular compartments and returned back to the plasma membrane. In the present study, we used the cell surface protein biotinylation approach to assess whether SIN-1 alters the rates of either internalization or reinsertion of CHT protein at the plasma membrane. After biotinylation of cell surface proteins at 4°C in the absence of SIN-1, the profiles for CHT internalization were compared in cells incubated at 37°C in the absence (control) or presence of 1 mM SIN-1 for 5 and 15 min; after this incubation, residual biotin was stripped from proteins that remained at the cell surface to ensure that only internalized biotinylated proteins were detected.

Importantly, the data illustrated in Fig. 7 reveal a statistically significant increase in the amount of CHT protein internalized from the plasma membrane in SIN-1-treated SH-SY5Y-CHT cells compared with vehicle-treated control cells. At both 5 and 15 min after the addition of 1 mM SIN-1 to cells at 37°C, the levels of biotinylated CHT were greater than that found in control cells at 37°C (Fig. 7A, bottom, lane 3 versus lane 5, and lane 4 versus lane 6; $p < 0.001$ and $p < 0.05$, respectively); an immunoblot of the total cell levels of CHT is shown in Fig. 7A (top) to demonstrate equivalent expression of CHT in each group. The amount of internalized biotinylated CHT was normalized to total cell surface levels of biotinylated CHT in cells incubated at 4°C in the absence of SIN-1 (Fig. 7A, bottom, lane 1). As experimental controls to validate the method, 1) the amount of total cell surface CHT that is biotinylated is shown in Fig. 7A (bottom, lane 1), and 2) one dish of cells was incubated on ice to show that internalization of the protein was negligible at 4°C (data not shown) and that MesNa efficiently stripped biotin from cell surface proteins (Fig. 7A, bottom, lane 2). Typically, one CHT-immunoreactive band with molecular mass of approximately 50 kDa was found on immunoblots of SH-SY5Y-CHT cell lysates (Fig. 7A, top), in contrast to results obtained with HEK 293-CHT cell lysates (Fig. 5A, bottom). Biotinylated CHT from SH-SY5Y-CHT cells corresponded to the immunoreactive CHT band at approximately 50 kDa, similar to that seen with HEK 293-CHT cells.

A line graph summarizing data from multiple experiments is given in Fig. 7B showing an approximately 3-fold increase in the amount of internalized CHT in SIN-1-treated cells at 5 min (30 ± 0.3%) compared with control (10 ± 2.8%) ($p < 0.001$). Although still significantly different ($p < 0.05$), the

magnitude of the difference between control and SIN-1-treated cells was less at 15-min incubation under conditions that are permissive for CHT internalization. It is noteworthy that the amount of CHT internalized in control cells increased by approximately 2-fold from 5 to 15 min ($p < 0.05$). By comparison, the amount of CHT internalized in SIN-1-treated cells did not increase significantly from 5 to 15 min. These data suggest that the initial rate of internalization of CHT is enhanced by exposure of cells to SIN-1, but that this enhancement is not sustained as indicated by saturation of internalization at 15 min compared with control cells.

SIN-1 Effect on CHT Movement between Cell Surface and Subcellular Organelles. Some cell surface solute transporters and receptors traffic repeatedly between the cytoplasm and plasma membrane (Deken et al., 2003; Loder and Melikian, 2003). We demonstrate here, for the first time, that biotinylated CHT that has undergone internalization from the cell surface can be returned constitutively back to the plasma membrane (Fig. 8A). Figure 8B illustrates that, under the experimental conditions tested, approximately 40% of internalized biotinylated CHT returned to the cell surface by 15 min. Moreover, compared with vehicle-treated control cells, the rate of return of internalized CHT back to the cell surface was not altered in SIN-1-treated cells.

Effect of SIN-1 On Intracellular Oxidative Stress. To assess whether SIN-1 and its product $ONOO^-$ cause an increase in intracellular oxidative stress, the cell-permeable nonfluorescent probe DCFH-DA was used to monitor levels of reactive oxygen species in control, H_2O_2-, and SIN-1–treated cells. After diffusing into cells, the diacetate moiety is cleaved from DCFH by cytoplasmic esterases, and with increasing oxidative stress in cells DCFH can be oxidized to the fluorescent compound DCF. As shown in Fig. 9, both 500 μM H_2O_2 and 100 μM SIN-1 significantly increased the fluorescence intensity of DCF, confirming that they are membrane-permeable oxidizing agents; induction of DCF fluorescence was greater with SIN-1, suggesting that it is a more powerful oxidizing agent than is H_2O_2. Pretreatment with 100 U/ml catalase, which breaks down H_2O_2, attenuated increases in DCF fluorescence in cells treated with H_2O_2, but not in cells treated with SIN-1. These data indicate that the effects of SIN-1 on CHT were not likely to be mediated by or related to the formation of H_2O_2. In contrast, treatment of cells with either 100 U/ml SOD or 25 μM FeTPPS, which catalyze the decomposition of $ONOO^-$, significantly reduced the SIN-1-induced increase in DCF fluorescence, supporting the role of $ONOO^-$ in SIN-1 effects on CHT.

Nitration of Tyrosine Residues in CHT. To determine whether susceptible tyrosine residues in CHT undergo nitration in SIN-1-treated SH-SY5Y-CHT cells, we recovered FLAG-tagged CHT proteins from control and treated cell lysates by immunoprecipitation with anti-nitrotyrosine antibodies. Using experimental conditions where SIN-1 reduces CHT activity, we did not find evidence for tyrosine nitration in CHT proteins in cells treated with either SIN-1 or $ONOO^-$ (data not shown). The converse experiment was also performed in which CHT proteins were immunoprecipitated with anti-CHT antibodies and then probed on immunoblot with anti-nitrotyrosine antibodies. No evidence of nitration of CHT in SIN-1-treated cells was observed (data not shown).

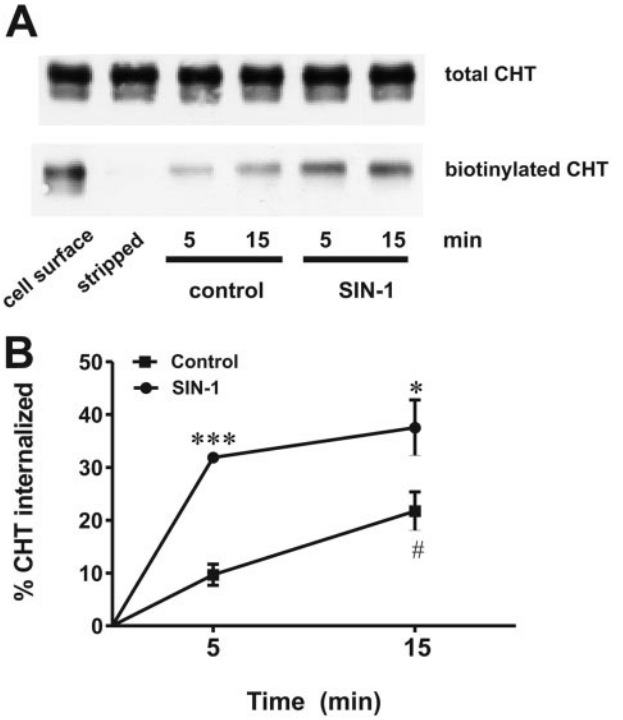

Fig. 7. SIN-1 increases internalization of CHT from the plasma membrane to subcellular compartments in differentiated SH-SY5Y-CHT cells. A, this representative immunoblot (bottom) shows increased internalization of biotinylated CHT at 5 and 15 min after addition of 1 mM SIN-1 compared with control cells. B, line graph displays CHT internalization data normalized to total cell surface CHT computed from four independent experiments. *, $p < 0.05$ and ***, $p < 0.001$, data are significantly different from controls, and #, $p < 0.05$ indicates a statistically significant difference for CHT internalization between 5- and 15-min values in control cells only.

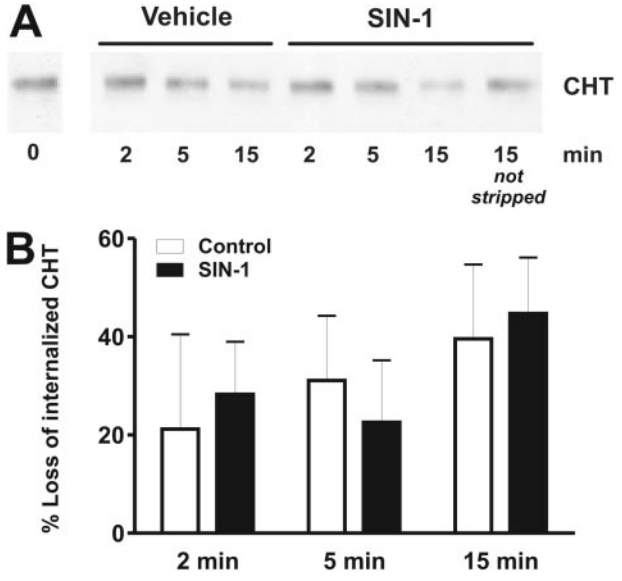

Fig. 8. Determination of the return of internalized CHT to the cell surface. After allowing internalization (37°C) for 15 min, two parallel groups of cells were chilled and incubated with MesNa at 4°C to strip biotin from proteins at the cell surface. Cells were then transferred to 37°C, and they were incubated in the presence or absence of 1 mM SIN-1. The decrement in intensity of the internalized, biotinylated CHT band with increasing incubation time (0, 2, 5, and 15 min) at 37°C represents the rate of CHT return back to the plasma membrane. A, data from a representative experiment are shown. B, histogram compiles data from three independent experiments, with data expressed as the percentage of loss of internalized CHT at each time point, thus allowing assessment of the return of CHT to the cell surface.

Effects of SIN-1 on Membrane Potential. As the velocity of choline uptake by CHT is coupled to the sodium electrochemical gradient, we tested the hypothesis that the inhibitory effect of SIN-1 on CHT activity is related to changes in membrane potential of the cell caused by inhibition of Na^+/K^+-ATPase and collapse of transmembrane ionic gradients. Previous studies demonstrated that Na^+/K^+-ATPase activity is decreased substantially by both SIN-1 and $ONOO^-$ (Guzman et al., 1995). To test this hypothesis, the effect of SIN-1 on membrane potential of SH-SY5Y cells was evaluated using the bis-oxonal dye. As illustrated in Fig. 10, bis-oxonal fluorescence was not different between vehicle-treated cells and cells treated for 30 min with 1 mM SIN-1. By comparison, treatment of cells with the Na^+/K^+-ATPase inhibitor ouabain (1 mM) resulted in increased bis-oxonal fluorescence, suggesting that cells are more depolarized.

Discussion

Several novel observations relating to the regulation of CHT function were made in this study: 1) cell surface levels of CHT are reduced by SIN-1 with this correlating to decreased choline uptake activity and HC-3 binding; 2) SIN-1 enhances the rate of internalization of CHT proteins from plasma membrane to subcellular compartments; similar enhancement of internalization of TfR in SIN-1-treated cells was also observed; 3) CHT that has undergone internalization from the plasma membrane to subcellular organelles can return back to the cell surface with the rate of this not altered by SIN-1; 4) SIN-1 effects on CHT function are not related to nitration of tyrosine residues in the protein or to changes in membrane potential that serves as a driving force for solute transport, and 5) RA-mediated differentiation of SH-SY5Y-CHT cells leads to an approximately 5-fold increase in CHT activity and protein content in cells.

Studying biological effects of $ONOO^-$ in cultured cells is technically challenging due to its short half-life (<1 s at physiological pH) (Radi et al., 2001), thus making the effective exposure time brief and making it difficult to attain the desired dose. Effects of a bolus of $ONOO^-$ may differ from what occurs in vivo where $ONOO^-$ is formed slowly and continuously. As an alternative to using $ONOO^-$ directly,

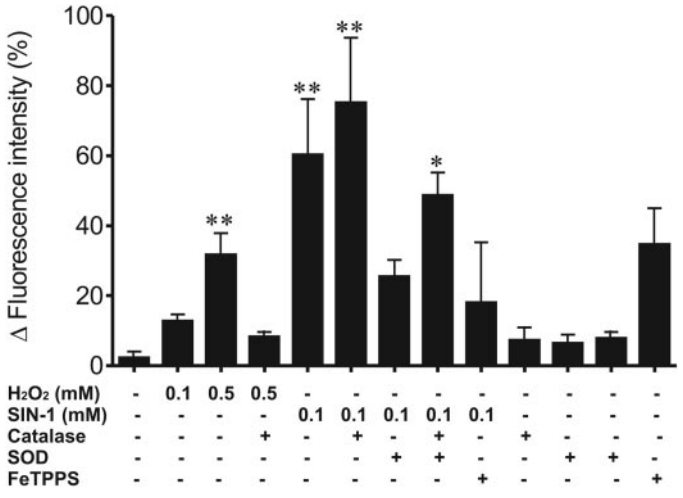

Fig. 9. DCF assay. HEK 293-CHT cells were incubated with 50 μM DCFH-DA for 1 h at 37°C. After washing away excess extracellular DCFH-DA, cells were treated with 100 and 500 μM H_2O_2 or 100 μM SIN-1, and the changes in fluorescence intensity were monitored at 5-min intervals for 30 min (excitation, 485 nm and emission, 510 nm). SOD, catalase, and FeTPPS were added to some samples at 5 min before the treatment. Changes in fluorescence were calculated according to the equation $\Delta F = (F_{t30} - F_{t0})/F_{t0} \times 100$. As expected, SIN-1 is a more powerful oxidizing agent than is H_2O_2. Catalase (100 units/ml) significantly reduced the oxidation of DCF in H_2O_2 (500 μM) treated-cells, but it had no effect in cells treated with SIN-1. However, 100 units/ml SOD, which react with O_2^- then inhibits the formation of $ONOO^-$, and 25 μM FeTPPS, an $ONOO^-$. scavenger, effectively lowered the oxidation of DCF in cells exposed to SIN-1. The bar graphs shown are means ± S.E.M. (n = 4). *, $p < 0.05$ and **, $p < 0.01$ compared with control cells.

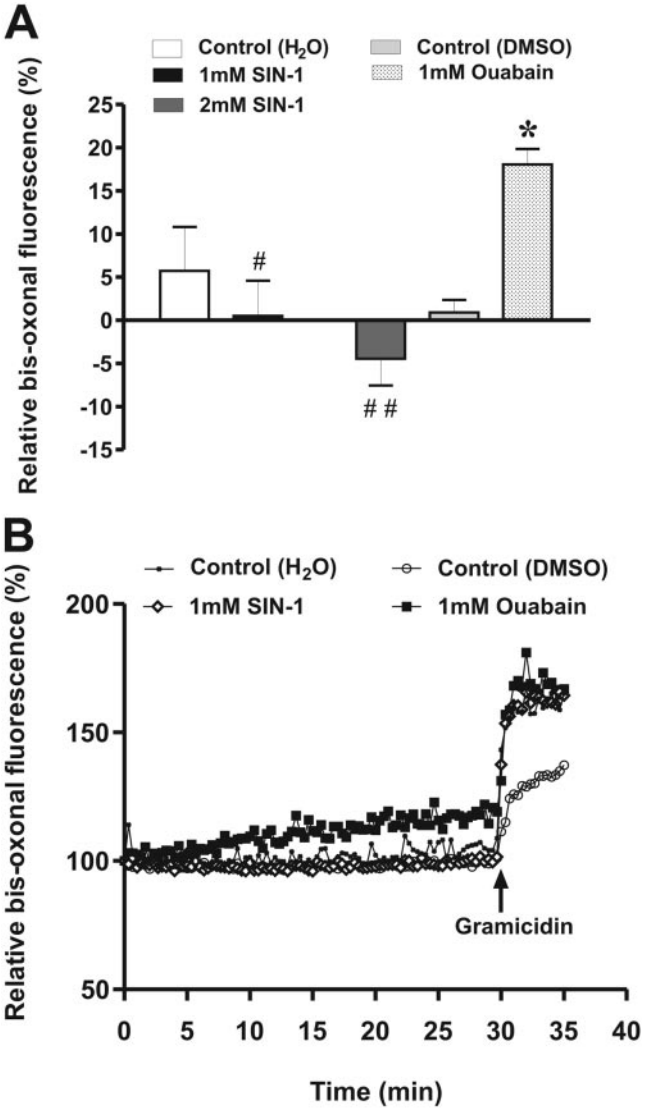

Fig. 10. SIN-1 did not alter cell plasma membrane potential when investigated using bis-oxonal. Cell suspensions were incubated in KRH buffer, pH7.4, containing 0.5 μM bis-oxonal for 30 min at 25°C. Bis-oxonal fluorescence was monitored as a function of time at wavelengths of 490 nm (excitation) and 530 nm (emission) using a PTI fluorescence spectrophotometer. When the baseline had stabilized, vehicle or drug (SIN-1 or ouabain) was added, and the fluorescence signal was observed continuously for 30 min. A, bar graph represents mean ± S.E.M. of data obtained from three independent experiments. B, representative traces of changes in fluorescence observed during a 30-min incubation with vehicle or drug treatment of cells. Drug or vehicle were added at time = 0 min on these traces, with the baseline having stabilized for several minutes before these additions. Gramicidine (10 μM) was added at the end of each incubation (i.e., at the 30-min time point) to induce membrane depolarization and observed as a large increase in fluorescence intensity.

SIN-1 (active metabolite of molsidomine) releases equimolar NO and O_2^-, leading to $ONOO^-$ generation in well oxygenated aqueous solution at physiological pH. This slow continuous production of $ONOO^-$ from SIN-1 resembles processes occurring during inflammation, ischemic injury and excitotoxicity (Darley-Usmar et al., 1992; Li et al., 2002).

It was reported previously that $ONOO^-$ and SIN-1 inhibit high-affinity choline uptake and ACh synthesis in cholinergic synaptosomes (Guermonprez et al., 2001), but the underlying mechanisms were not investigated. The present study shows that short-term exposure of HEK 293 and SH-SY5Y cells expressing CHT to 1 mM SIN-1 rapidly inhibits choline uptake to approximately 50% of control levels; this agrees with a previous report where synaptosomal HC-sensitive choline uptake was decreased to 50% of control by 0.8 mM SIN-1 (Guermonprez et al., 2001). We observed that the inhibitory effect of SIN-1 on CHT activity plateaus within minutes and remains stable up to 2 h. The reason for this is unclear, but as SIN-1 consumes molecular O_2 with NO generation this could potentially deplete O_2 in media, thereby limiting the maximal effect of SIN-1. Studies on the dynamics of O_2 consumption relative to NO production from SIN-1 have been published (Feelisch et al., 1989; Ullrich et al., 1997), but the time frame for substantial reduction of O_2 in media occurs over hours rather than a few minutes.

Inhibition of HC-sensitive choline uptake by SIN-1 in both non-neural (HEK 293) and neural (SH-SY5Y) cells indicates that the effect is not cell type-specific. However, comparison of HEK 293-CHT and RA-differentiated SH-SY5Y-CHT cells revealed a difference in sensitivity of cells to inhibitory effects of SIN-1 on CHT activity. Although the redox state of HEK 293 and differentiated SH-SY5Y cells was not addressed in this study, both cellular redox state and GSH levels are important defenses against $ONOO^-$ and SIN-1 (Barker et al., 1996; Fass et al., 2004). It is noteworthy that RA treatment can protect PC12 cells from oxidative injury generated by H_2O_2 (Jackson et al., 1991), suggesting that the transition of SH-SY5Y cells to a more differentiated state may contribute to differences in sensitivity of CHT to SIN-1 between HEK 293 and SH-SY5Y cells.

Characteristics of choline uptake measured in SH-SY5Y-CHT cells are similar to those reported in other expression systems such as *Xenopus laevis* oocytes and transiently transfected cells. Strikingly, RA-induced differentiation of SH-SY5Y-CHT cells markedly enhances CHT activity and protein levels in parallel with morphological differentiation of the cells. As stable introduction of transgenes into recipient cells using traditional plasmid transfection methods normally results in random integration of the gene into the host genome, the effects of RA-induced differentiation was tested on two separate clonal cell lines. The data show that both cell lines respond similarly to RA, suggesting that it is unlikely that the integration site of CHT cDNA is responsible for the RA-induced increase in CHT expression. Further studies are required to elucidate mechanisms by which RA enhances CHT activity and protein levels in SH-SY5Y-CHT cells.

To assess whether SIN-1 and its product $ONOO^-$ cause intracellular oxidative stress, the cell-permeable probe DCFH-DA was used (Crow, 1997; Martin-Romero et al., 2004). Coupling DCFH measures with oxidant inhibitors and scavengers makes it possible to assess oxidant potency and to identify the oxidant mediating SIN-1 effects. Oxidation of nonfluorescent DCFH to its fluorescent product DCF is relatively selective for $ONOO^-$ compared with O_2^-, H_2O_2, or NO, thereby allowing $ONOO^-$ formation to be monitored. Under the experimental conditions used, it seems that the product of SIN-1 decomposition is $ONOO^-$ rather than H_2O_2; catalase (scavenger of H_2O_2) effectively abolished increased DCF oxidation by H_2O_2, but it did not alter increased fluorescence of DCF in the presence of SIN-1. The interpretation that SIN-1-induced $ONOO^-$ causes oxidative stress is supported by data that SOD (scavenges O_2^-) and FeTPPS (scavenges peroxynitrite and uncouples the reaction of NO with O_2 to decrease $ONOO^-$ formation) inhibited oxidation of DCF by SIN-1. In addition, because intracellular DCF is highly oxidized when SIN-1 is added to media, this indicates that intracellular oxidative stress might contribute to SIN-1 effects. DCF fluorescence induced by SIN-1 is severalfold greater than the response to H_2O_2, confirming the potency of pro-oxidant $ONOO^-$.

A primary effect of $ONOO^-$ on proteins is nitration of tyrosine residues (Beckman et al., 1992). In relation to this, nitrotyrosine immunoreactivity is increased in necropsy AD brain (Smith et al., 1997), indicating that $ONOO^-$ may be involved in the disease pathogenesis. Nitrated residues disrupt normal protein function by several mechanisms, such as altering its ability to undergo tyrosine phosphorylation (Berlett et al., 1996; Nomiyama et al., 2004), modification of protein conformation (Hodara et al., 2004; Reynolds et al., 2005) and altering susceptibility to proteolysis (Hodara et al., 2004; Bar-Shai and Reznick, 2006). We hypothesized that tyrosine nitration in CHT may induce loss-of-function. Rat CHT contains 31 tyrosines that are potential targets for $ONOO^-$-mediated nitration; 12 tyrosines are located in transmembrane domains and 19 are arrayed in extracellular and intracellular loops. Tyrosine nitration in target proteins yields a modification that can be detected immunologically; thus, we used anti-nitrotyrosine antibodies to analyze CHT immunoprecipitated from SIN-1-treated cells. We did not find evidence of nitration of tyrosines in CHT. Similar results (i.e., absence of nitrotyrosine-immunoreactive bands after SIN-1 and $ONOO^-$ treatment) were found with cholinergic synaptosomes or cell lines that overexpress the human dopamine transporter that were exposed to high doses of SIN-1 (Guermonprez et al., 2001; Park et al., 2002). An alternative target in CHT for $ONOO^-$ could be oxidation of cysteine thiols.

We show for the first time that SIN-1 decreases choline uptake by increasing CHT internalization without altering its return to plasma membrane, thus lowering cell surface CHT. Cell surface CHT is determined by its internalization rate into endosomal compartments and by the rate of movement of previously internalized or new CHT to plasma membrane. This latter event is critical for increasing cell surface CHT to mediate rapid enhancement of choline uptake after ACh release, thus facilitating transmitter synthesis to maintain neurotransmission (Ferguson and Blakely, 2004; Ribeiro et al., 2006). Dynamic movement of CHT between plasma membrane and cellular organelles in neurons may involve both regulated and constitutive mechanisms with different functional roles (Ribeiro et al., 2006). In this model, constitutive exocytosis-endocytosis maintains a pool of plasma membrane transporters (estimated at 15% of total CHT), whereas regulated exocytosis of synaptic vesicles delivers CHT to the cell surface during prolonged excitation of cholin-

ergic nerve terminals. An intracellular recycling pool of CHT that can be recruited as needed could explain how cholinergic transmission is maintained during long periods of stimulation (Birks and MacIntosh, 1961). Conversely, changes that enhance CHT internalization and/or decrease its return to plasma membrane could decrease its cell surface levels, lower ACh synthesis and comprise cholinergic communication.

The mechanism by which SIN-1 enhances CHT internalization is unknown, but may involve modification of CHT interaction with cellular proteins and/or endocytic machinery such as adaptor, Rab or clathrin-pathway proteins. After internalization in clathrin-coated pits, CHT seems to be directed to early endosomes as it colocalizes with Rab5 shortly after endocytosis (Ribeiro et al., 2005). In addition to its role in endosomal transport, Rab5 may participate in synaptic vesicle recycling/formation and modulate synaptic vesicle-mediated mobilization of CHT, thus regulating choline uptake (Ferguson et al., 2003; Ribeiro et al., 2003). In this study, SIN-1 also increased TfR internalization from plasma membrane similar to the effect on CHT. TfR is endocytosed by a clathrin-mediated process (Hanover et al., 1985), and although it was shown that SIN-1 decreases cell surface TfR levels (Richardson et al., 1995), a relationship between these events has not been reported. Taken together, our findings suggest that this SIN-1-mediated effect is not specific to CHT, but that it may be generalized to other cell surface proteins that undergo regulated endocytosis by a clathrin-mediated mechanism.

Acknowledgments

We thank Drs. Jeffrey Dixon and Stephen Sims for assistance with, and use of, the Photon Technology International fluorescence spectrophotometer for monitoring changes in cell membrane potential.

References

Apparsundaram S, Ferguson SM, and Blakely RD (2001) Molecular cloning and characterization of a murine hemicholinium-3-sensitive choline transporter. *Biochem Soc Trans* **29:**711–716.

Apparsundaram S, Martinez V, Parikh V, Kozak R, and Sarter M (2005) Increased capacity and density of choline transporters situated in synaptic membranes of the right medial prefrontal cortex of attentional task-performing rats. *J Neurosci* **25:**3851–3856.

Bar-Shai M and Reznick AZ (2006) Reactive nitrogen species induce nuclear factor-kappaB-mediated protein degradation in skeletal muscle cells. *Free Radic Biol Med* **40:**2112–2125.

Barker JE, Heales SJ, Cassidy A, Bolanos JP, Land JM, and Clark JB (1996) Depletion of brain glutathione results in a decrease of glutathione reductase activity; an enzyme susceptible to oxidative damage. *Brain Res* **716:**118–122.

Baskey JC, Colhoun EH, and Rylett RJ (1990) Cholinergic but not GABAergic neuronal markers are decreased in primary neuronal cultures treated with choline mustard. *Brain Res* **519:**209–216.

Beckman JS (1994) Peroxynitrite versus hydroxyl radical: the role of nitric oxide in superoxide-dependent cerebral injury. *Ann N Y Acad Sci* **738:**69–75.

Beckman JS, Ischiropoulos H, Zhu L, von der Woerd M, Smith C, Chen J, Harrison J, Martin JC, and Tsai (1992) Kinetics of superoxide dismutase- and iron-catalyzed nitration of phenolics by peroxynitrite. *Arch Biochem Biophys* **298:**438–445.

Berlett BS, Friguet B, Yim MB, Chock PB, and Stadtman ER (1996) Peroxynitrite-mediated nitration of tyrosine residues in *Escherichia coli* glutamine synthetase mimics adenylylation: relevance to signal transduction. *Proc Natl Acad Sci U S A* **93:**1776–1780.

Birks RI and MacIntosh FC (1961) Acetylcholine metabolism of a sympathetic ganglion. *Can J Biochem Physiol* **39:**787–827.

Bryan-Lluka LJ, Papacostas MH, Paczkowski FA, and Wanstell JC (2004) Nitric oxide donors inhibit 5-hydroxytryptamine (5-HT) uptake by the human 5-HT transporter (SERT). *Br J Pharmacol* **143:**63–70.

Calderón FH, Bonnefont A, Munoz FJ, Fernandez V, Videla LA, and Inestrosa NC (1999) PC12 and neuro 2a cells have different susceptibilities to acetylcholinesterase-amyloid complexes, amyloid25–35 fragment, glutamate, and hydrogen peroxide. *J Neurosci Res* **56:**620–631.

Chatterjee TK, Cannon JG, and Bhatnagar RK (1987) Characteristics of [^{3}H]hemicholinium-3 binding to rat striatal membranes: evidence for negative cooperative site-site interactions. *J Neurochem* **49:**1191–1201.

Crow JP (1997) Dichlorodihydrofluorescein and dihydrorhodamine 123 are sensitive indicators of peroxynitrite in vitro: implications for intracellular measurement of reactive nitrogen and oxygen species. *Nitric Oxide* **1:**145–157.

Darley-Usmar VM, Hogg N, O'Leary VJ, Wilson MT, and Moncada S (1992) The simultaneous generation of superoxide and nitric oxide can initiate lipid peroxidation in human low density lipoprotein. *Free Radic Res Commun* **17:**9–20.

Deken SL, Wang D, and Quick MW (2003) Plasma membrane GABA transporters reside on distinct vesicles and undergo rapid regulated recycling. *J Neurosci* **23:**1563–1568.

Encinas M, Iglesias M, Llechna N, and Comella JX (1999) Extracellular-regulated kinases and phosphatidylinositol 3-kinase are involved in brain-derived neurotrophic factor-mediated survival and neuritogenesis of the neuroblastoma cell line SH-SY5Y. *J Neurochem* **73:**1409–1421.

Fass U, Panickar K, Williams K, Nevels K, Personett D, and McKinney M (2004) The role of glutathione in nitric oxide donor toxicity to SN56 cholinergic neuron-like cells. *Brain Res* **1005:**90–100.

Ferguson SM, Bazalakova M, Savchenko V, Tapia JC, Wright J, and Blakely RD (2004) Lethal impairment of cholinergic neurotransmission in hemicholinium-3-sensitive choline transporter knockout mice. *Proc Natl Acad Sci U S A* **101:**8762–8767.

Ferguson SM, Savchenko V, Apparsundaram S, Zwick M, Wright J, Heilman CJ, Yi H, Levey AI, and Blakely RD (2003) Vesicular localization and activity-dependent trafficking of presynaptic choline transporters. *J Neurosci* **23:**9697–9709.

Ferguson SM and Blakely RD (2004) The choline transporter resurfaces: new roles for synaptic vesicles? *Mol Interv* **4:**22–37.

Feelisch M, Ostrowski J, and Noack E (1989) On the mechanism of NO release from sydnonimines. *J Cardiovasc Pharmacol* **14 (Suppl 11):**S13–S22.

Gates J Jr, Ferguson SM, Blakely RD, and Apparsundaram S (2004) Regulation of choline transporter surface expression and phosphorylation by protein kinase C and protein phosphatase 1/2A. *J Pharmacol Exp Ther* **310:**536–545.

Guermonprez L, Ducrocq C, and Gaudry-Talarmain TM (2001) Inhibition of acetylcholine synthesis and tyrosine nitration induced by peroxynitrite are differentially prevented by antioxidants. *Mol Pharmacol* **60:**838–846.

Guzman NJ, Fang MZ, Tang SS, Ingelfinger JR, and Garg LC (1995) Autocrine inhibition of Na^+/K^+-ATPase by nitric oxide in mouse proximal tubule epithelial cells. *J Clin Invest* **95:**2083–2088.

Haga T and Noda H (1973) Choline uptake systems of rat brain synaptosomes. *Biochim Biophys Acta* **291:**564–575.

Hanover JA, Beguinot L, Willingham MC, and Pastan IH (1985) Transit of receptors for epidermal growth factor and transferrin through clathrin-coated pits. Analysis of the kinetics of receptor entry. *J Biol Chem* **260:**15938–15945.

Hodara R, Norris EH, Giasson BI, Mishizen-Eberz AJ, Lynch DR, Lee VM, and Ischiropoulos H (2004) Functional consequences of alpha-synuclein tyrosine nitration: diminished binding to lipid vesicles and increased fibril formation. *J Biol Chem* **279:**47746–47753.

Huang CL, Huang NK, Shyue SK, and Chern Y (2003) Hydrogen peroxide induces loss of dopamine transporter activity: a calcium-dependent oxidative mechanism. *J Neurochem* **86:**1247–1259.

Jackson GR, Morgan BC, Werrbach-Perez K, and Perez-Polo JR (1991) Antioxidant effect of retinoic acid on PC12 rat pheochromocytoma. *Int J Dev Neurosci* **9:**161–170.

Kukkonen JP, Hautala R, and Akerman KE (1996) Muscarinic depolarization of SH-SY5Y human neuroblastoma cells as determined using oxonol V. *Neurosci Lett* **212:**57–60.

Li CQ, Trudel LJ, and Wogan GN (2002) Genotoxicity, mitochondrial damage, and apoptosis in human lymphoblastoid cells exposed to peroxynitrite generated from SIN-1.*Chem Res Toxicol* **15:**527–535.

Lips KS, Pfeil U, Haberberger RV, and Kummer W (2002) Localisation of the high-affinity choline transporter-1 in the rat skeletal motor unit. *Cell Tissue Res* **307:**275–280.

Loder MK and Melikian HE (2003) The dopamine transporter constitutively internalizes and recycles in a protein kinase C-regulated manner in stably transfected PC12 cell lines. *J Biol Chem* **278:**22168–22174.

Martin-Romero FJ, Gutierrez-Martin Y, Henao F, and Gutierrez-Merino C (2004) Fluorescence measurements of steady state peroxynitrite production upon SIN-1 decomposition: NADH versus dihydrodichlorofluorescein and dihydrorhodamine 123. *J Fluoresc* **14:**17–23.

Nakata K, Okuda T, and Misawa H (2004) Ultrastructural localization of high-affinity choline transporter in the rat neuromuscular junction: enrichment on synaptic vesicles. *Synapse* **53:**53–56.

Nomiyama T, Igarashi Y, Taka H, Mineki R, Uchida T, Ogihara T, Choi JB, Uchino H, Tanaka Y, Maegawa H, et al. (2004) Reduction of insulin-stimulated glucose uptake by peroxynitrite is concurrent with tyrosine nitration of insulin receptor substrate-1. *Biochem Biophys Res Commun* **320:**639–647.

Okuda T, Haga T, Kanai Y, Endou H, Ishihara T, and Katsura I (2000) Identification and characterization of the high-affinity choline transporter. *Nat Neurosci* **3:**120–125.

Okuda T, Okamura M, Kaitsuka C, Haga T, and Gurwitz D (2002) Single nucleotide polymorphism of the human high affinity choline transporter alters transport rate. *J Biol Chem* **277:**45315–45322.

Park SU, Ferrer JV, Javitch JA, and Kuhn DM (2002) Peroxynitrite inactivates the human dopamine transporter by modification of cysteine 342: potential mechanism of neurotoxicity in dopamine neurons. *J Neurosci* **22:**4399–4405.

Radi R, Peluffo G, Alvarez MN, Naviliat M, and Cayota A (2001) Unraveling peroxynitrite formation in biological systems. *Free Radic Biol Med* **30:**463–488.

Reynolds MR, Berry RW, and Binder LI (2005) Site-specific nitration differentially influences tau assembly in vitro. *Biochemistry* **44:**13997–14009.

Ribeiro FM, Alves-Silva J, Volknandt W, Martins-Silva C, Mahmud H, Wilhelm A, Gomez MV, Rylett RJ, Ferguson SS, Prado VF, et al. (2003) The hemicholinium-3 sensitive high affinity choline transporter is internalized by clathrin-mediated endocytosis and is present in endosomes and synaptic vesicles. *J Neurochem* **87:**136–146.

Ribeiro FM, Black SA, Cregan SP, Prado VF, Prado MA, Rylett RJ, and Ferguson SS (2005) Constitutive high-affinity choline transporter endocytosis is determined by a carboxyl-terminal tail dileucine motif. *J Neurochem* **94:**86–96.

Ribeiro FM, Black SAG, Rylett RJ, Prado VF, Ferguson SSG, and Prado MAM (2006) The 'ins' and 'outs' of the high-affinity choline transporter CHT1. *J Neurochem* **97:**1–12.

Richardson DR, Neumannova V, Nagy E, and Ponka P (1995) The effect of redox-related species of nitrogen monoxide on transferrin and iron uptake and cellular proliferation of erythroleukemia (K562) cells. *Blood* **86:**3211–3219.

Smith MA, Richey Harris PL, Sayre LM, Beckman JS, and Perry G (1997) Widespread peroxynitrite-mediated damage in Alzheimer's disease. *J Neurosci* **17:** 2653–2657.

Tran MH, Yamada K, Nakajima A, Mizuno M, He J, Kamei H, and Nabeshima T (2003) Tyrosine nitration of a synaptic protein synaptophysin contributes to amyloid beta-peptide-induced cholinergic dysfunction. *Mol Psychiatry* **8:**407–412.

Truckenmiller ME, Vawter MP, Cheadle C, Coggiano M, Donovan DM, Freed WJ, and Becker KG (2001) Gene expression profile in early stage of retinoic acid-induced differentiation of human SH-SY5Y neuroblastoma cells. *Restor Neurol Neurosci* **18:**67–80.

Ullrich T, Oberle S, Abate A, and Schroder H (1997) Photoactivation of the nitric oxide donor SIN-1. *FEBS Lett* **406:**66–68.

Yamamura HI and Snyder SH (1973) High affinity transport of choline into synaptosomes of rat brain. *J Neurochem* **21:**1355–1374.

Address correspondence to: Dr. Rebecca Jane Rylett, Department of Physiology and Pharmacology, Schulich School of Medicine and Dentistry, University of Western Ontario, London, ON, Canada N6A 5C1. E-mail: jane.rylett@schulich.uwo.ca